STIMULATED RAMAN SCATTERING IN HYDROGEN

CHANG-TSANG WILLIAM HSIEH

STIMULATED RAMAN SCATTERING IN HYDROGEN

by

© Chang-Tsang William Hsieh

Submitted in partial fulfillment of the requirements for the degree of Master of Science Memorial University of Newfoundland

March, 1973

STIMULATED RAMAN SCATTERING IN HYDROGEN

ABSTRACT

An experimental investigation to determine the threshold powers for stimulated Raman scattering in compressed hydrogen at room temperature will be presented. The pressure range of the hydrogen gas was from approximately 2 to 28 atm. Ruby laser light up to 120 MW was used as the incident beam. Both linearly and circularly polarized light were used. It was found that circularly polarized light could stimulate the rotational Raman, $S_0(1)$, line as well as the vibrational Raman, $Q_1(1)$, line while linearly polarized light could only give rise to the stimulated $Q_1(1)$ line in the present power range. It was also found that the threshold power for the stimulated $Q_1(1)$ line is higher for circularly polarized light than for linearly polarized light. The threshold power of the stimulated $Q_1(1)$ line by linearly polarized light was found to depend on the gas density in general agreement with the theory. On the other hand, the threshold power of both stimulated $S_0(1)$ and stimulated $Q_1(1)$ lines by circularly polarized light agreed with theory only when the effect of a competing nonlinear process with a gain dependent on gas density was included.

CONTENTS

LIST OF TABLES

LIST OF FIGURES

CHAPTER I

INTRODUCTION

Since the early days of study of nonlinear optical phenomena by means of pulsed high intensity lasers, the Raman scattering in liquids and gases has received much attention. When a conventional light source is used, the intensity of Raman lines in liquids is from 10^{-2} to 10^{-3} of that of the unshifted Rayleigh line, and in low pressure gases the ratio is typically 10^{-4}. The Raman scattered light in the forward direction which is stimulated by an intense laser beam, on the other hand, may acquire the intensity close to that of the exciting laser light.

The stimulated Raman scattering process was first observed accidentally by Woodbury and Ng[1] in nitrobenzene in 1962. Since then the stimulated Raman spectra of many solids, liquids, and gases have been studied by many investigators. The stimulated Raman spectrum has the following distinct characteristics: (a) If the spontaneous spectrum consists of several lines in a relatively small frequency range only the sharpest and the most intense one which is Stokes shifted is normally stimulated. (b) There exists a definite threshold power level of the exciting light beam above which the stimulated Raman scattering can occur.

(c) It shows the "gain narrowing", i.e. the linewidth of the stimulated Raman line is much narrower than that of the spontaneous Raman line. When the pump power is increased beyond the threshold value, the Stokes shifted line which appeared first will increase its intensity without creating other lines of the spontaneous Raman spectrum. Further increase in the pump power can, however, create higher order Stokes lines and anti-Stokes lines whose frequency shifts from the laser frequency represent integral multiples of the first stimulated Raman line. These higher order Stokes or anti-Stokes lines do not arise from normal Raman transitions involving new quantum states but from the nonlinear frequency mixing in the scattering medium. Although there are many papers which provide both classical and quantum mechanical theories for the stimulated Raman scattering, all of these theories are based on some simplified assumptions which often limit their usefulness in interpreting experimental results.

The stimulated Raman scattering in gaseous hydrogen and deuterium was first studied by Minck et al[2]. Minck et al[3] investigated the Raman spectra of D_2 at the constant density of 25 amagats as a function of gas temperature and laser polarization. In addition, they reported the observation of the stimulated rotational Raman line, $S_0(0)$, and stimulated rotational Raman lines of H_2 at 1 atmosphere and 80°K

using a laser beam of either linear or circular polarization.

Lallemand et al[4] studied the stimulated $Q_1(1)$ line of H_2 and Bloembergen et al[5] studied the stimulated $Q_1(1)$ and $S_0(1)$ lines of the same gas, both using linearly polarized light. They studied the nonlinear Raman gain versus gas density. The highlight of their results was the observation of some indication of Dicke narrowing at pressures below 20 amagats. The linewidth was found to reach a minimum at approximately 15 amagats of the gas density. The Dicke narrowing effect was previously reported in the H_2 quadrupole spectrum by Rank[6].

The present investigation was undertaken to study the relationship between the threshold power of the stimulated Raman lines, $Q_1(1)$ and $S_0(1)$, of H_2 in terms of gas density and incident laser polarization. Since the threshold power is inversely proportional to nonlinear gain coefficient, the study is designed to find the relationship between the nonlinear gain for the stimulated Raman lines of H_2 as a function of gas density, the dependence of the gain on the laser polarization, and any other relevant information which will be helpful for the understanding of the stimulated process in gaseous hydrogen.

CHAPTER II

EXPERIMENTAL APPARATUS AND PROCEDURE

1. Apparatus

(A) Laser System

A Korad Model K-1 giant pulse ruby laser system, Q-switched by means of a saturable dye solution, was used as the light source. A Czolchralski "standard" ruby rod doped with 0.05% chromium oxide (Cr_2O_3), 4 inch long and 9/16 inch in diameter with flat/flat ends, served as the active medium for the laser. Both end surfaces of the ruby rod were flat within 1/10 of a wavelength at wavelength 6943Å, the ruby laser wavelength, with anti-reflection coatings. End surfaces were parallel within 2 - 4 seconds of arc. A helical xenon flashlamp provided the optical pumping for the ruby rod. Both the rod and the flashlamp were cooled by means of a Brinkmann Lauda Model K-2/R circulator-cooler.

The optical cavity of the laser consisted of the front reflector, an optical flat sapphire disk 1" dia. X 1/8" thick with approximately 13% reflectivity for wavelength 6943Å, and the dye cell/rear reflector combination. The dye cell which contained the saturable dye solution, cryptocyanine in methanol, was made of two optical flat fused quartz disks joined by a ring-shaped quartz spacer 1/8" thick. On the top of the spacer of the cell a small hole was drilled,

which made it possible to vary the dye concentration inside the cell. The inside surface of the "outside" window of the dye cell, which served as the rear reflector of the optical cavity of the laser, was dielectric coated to give approximately 100% reflectivity for wavelength 6943 Å light. In addition, the outside surface of the "inside" window of the dye cell was anti-reflection coated to avoid the reflection loss.

The characteristics of the ruby laser output were: (i) a beam divergence of approximately 6 milliradians which is the manufacturer's specified value, (ii) a linewidth of 0.01 - 0.04 cm^{-1} which was determined previously by Hsu[7] using a Fabry-Perot interferometer, (iii) a pulse width of 18 ± 5 nanoseconds and (iv) a maximum pulse energy of 2.0 joules.

(B) Diagnostics

The layout of the diagnostic components is shown schematically in Fig. 1. The laser beam from the ruby laser partially reflected off the beam splitter, S_1, was monitored by an ITT F-4000 photodiode in conjunction with a Tektronix 519 oscilloscope. The temporal laser profile obtained from the oscilloscope was recorded photographically for each laser pulse used. Just in front of the hydrogen gas cell, as shown in Fig. 1, the second beam splitter, S_2, was placed

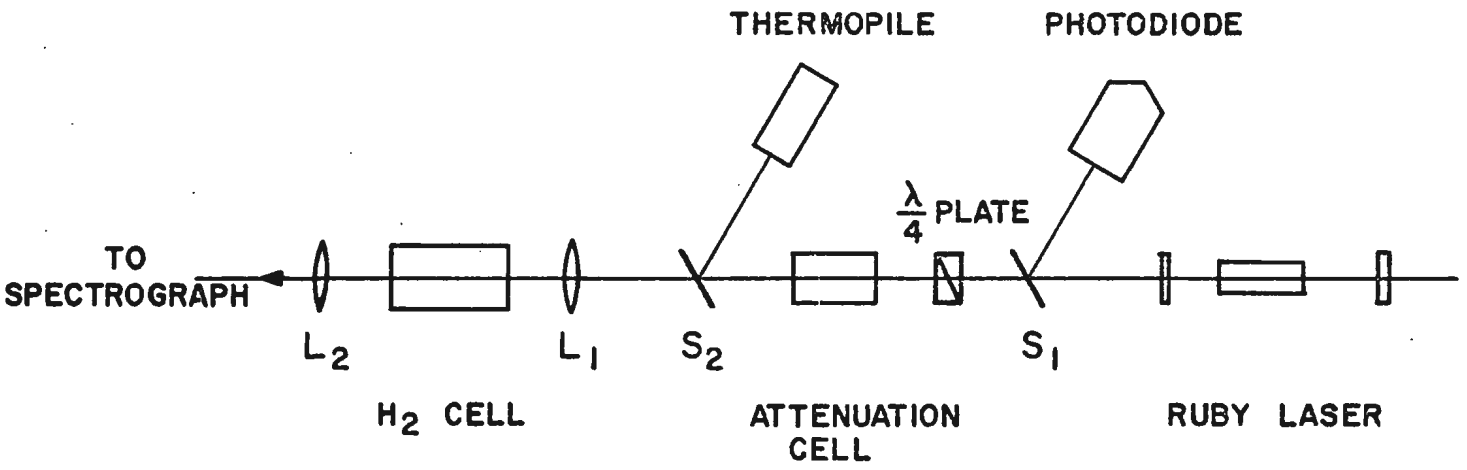

Fig. 1

Experimental Setup

to monitor the laser energy entering the cell. A TRG Model 100 thermopile in conjunction with a Keithley 150B Microvolt/Ammeter was used to determine the integrated laser energy. Microvolt output from the Keithley meter was continuously recorded by means of a Leeds & Northrup Speedomax G recorder.

(C) High Pressure Gas Cell and Spectrograph

A stainless steel high pressure gas cell with a side window designed and used for other experiments [7] was used to contain the compressed hydrogen gas. The straight through windows, entrance and exit windows, as well as the side viewing window were fused quartz disks 3/8" thick and 1 3/8" in diameter. The cell was originally designed to withstand pressures up to 2500 psi.

The spectra of the scattered light were photographed through a Jarrel-Ash 3.4 meter Ebert Spectrograph. An MIT plane diffraction grating with 590 lines/mm and 135 mm X 57 mm ruled area was used at 7th. order for the rotational Raman $S_o(1)$ line at wavelength 7238Å and 5th. order for the vibrational Raman $Q_1(1)$ line at wavelength 9759Å. Kodak 1 N plates were used to obtain the spectrograms.

2. Experimental Procedure

(A) Optical Arrangement

The light beam emerging from the ruby laser was focused into the gas cell as shown in Fig. 1. When a circularly polarized beam was required, a $\lambda/4$ plate which was made of a crystalline quartz, was placed immediately in front of the laser. The intensity of the laser light incident on the gas sample was varied by passing the laser beam through an attenuation cell containing a solution of copper sulfate in water at a desired concentration. Care was taken to ensure that the entrance window of the attenuation cell was placed perpendicular to the beam such that no angular deviation of light beam emerging from the cell should result. The condensing lens, L_1 (Fig. 1), 20 cm in focal length, was placed in front of the entrance window of the cell in such a way that the laser beam was brought into focus at the middle of the cell. The forward scattered beam emerging from the exit window of the cell was first collimated by means of the second lens, L_2 (Fig. 1), 20 cm in focal length, before it was refocused onto the slit of the spectrograph by means of 10 cm focal length lens. A piece of ground glass plate was used in front of the slit to obtain reasonably uniform slit illumination.

(B) Determination of the Power of the Laser Beam

The ruby laser power input to the gas cell was determined from the pulse width measured by the photodiode and the energy measured by the thermopile as described in Section 1. For the purpose of determining the power of the laser beam, the half-intensity full width of the temporal profile of a pulse was taken as the pulse width. The average power, P, of the laser beam incident on the gas cell was then calculated by the following relationship:

$$P = \frac{E}{t} \times 10^3$$

where P is in Megawatts, E is the energy in joules, t is the pulse width in nanoseconds. The power density (power per unit cross sectional area) at the focal region was calculated using a focal area of 0.011 cm^2, which was computed for a beam divergence of 6×10^{-3} radians and a 20 cm focal length condensing lens.

(C) Determination of Threshold Powers

Two different types of experiments were carried out to determine the threshold powers of the stimulated Raman lines at various gas pressures using linearly as well as circularly polarized incident light. For each of the first group of experiments ("constant pressure experiments"), the hydrogen gas pressure in the gas cell was kept constant while

the laser power input to the gas cell was varied in approximately equal steps either from higher to lower powers or vice versa, the spectrogram being taken at each step. Threshold power was then determined from the spectrogram. Each experiment was repeated at least twice to ascertain that the threshold values were consistent within the experimental error. Threshold powers were thus determined at various gas pressures ranging from approximately 2 to 28 atmospheres (25 to 415 psi). In order to check the validity of the threshold powers for different gas pressures the "constant power experiments" were performed. For each of these experiments, the laser power input to the gas cell was kept at a reasonably constant level while the hydrogen gas pressure was changed in certain steps. A total of 29 experiments were carried out in the present study, 22 in "constant pressure" experiments and 7 in "constant power" experiments.

The following possible sources of errors are considered for the determination of the threshold powers. Firstly, in the power measurement, the error for obtaining the values of incident laser energy is estimated to be approximately 5%, and those for determining the pulse width of the laser beam to be approximately 9%. The laser energy readings monitored by the calorimeter were calibrated against a Korad Model K-J calorimeter (manufacturer's stated accuracy of $\pm$3%) as described by Hsu[7]. The estimated error of 5% as stated

above, takes into consideration the accuracy of the monitoring calorimeter readings. The measurement of pulse widths, on the other hand, introduces errors from the distortion of temporal pulse profile by the measuring oscilloscope, and the measurement error in determining the half-intensity width of the pulse profile photographed. In measuring pulse widths from the oscillograms an uncertainty of ± 1.5 nanoseconds was typical for an average pulse of 18 nanoseconds. Consequently the total estimated error in power measurement is approximately 11%. Secondly, in determining appropriate threshold power from the oscillograms, the error can be estimated from the power increment between consecutive spectrograms taken at constant pressure. The power increment was typically 15% of the total power. Consequently the overall percentage error for the threshold power determination is estimated to be 19%. Any other possible systematic errors can not be estimated easily.

(D) Calibration of the Spectral Regions

The spectral regions for the stimulated Raman lines of hydrogen were calibrated using neon discharge emission lines. The calibration curves were obtained with the aid of a Gaertner comparator. The center position of the plate was set at wavelength 49,634Å in the first order, so that the 5th. order spectrum of the $Q_1(1)$ hydrogen Raman line and the

7th. order spectrum of the $S_o(1)$ hydrogen Raman line could be photographed simultaneously.

(E) Gas System

In this investigation the hydrogen gas (normal para/ortho ratio) from a commercial cylinder, supplied by Canadian Liquid Air Ltd., was used. An Ashcroft Bourdon-type pressure gauge was used to measure the gas pressure inside the cell. The pressure gauge was calibrated by means of an Ashcroft dead weight balance. Prior to introducing the hydrogen gas into the gas cell the system was evacuated. Since all the pressures used were below the cylinder pressure of hydrogen gas, the desired pressure inside the cell was obtained by introducing an appropriate amount of gas directly from the cylinder. Pressure range used in this investigation was from 25 to 415 psi. All the experiments were performed at room temperature.

The pressures of the gas were converted to densities in amagat units by using the known isothermal data[8].

CHAPTER III

THEORY OF STIMULATED RAMAN SCATTERING

1. Derivation of the Gain

This gain derivation is a brief summary of the work by R.M. Herman[9]. Consider a gas system which contains N molecules per unit volume. When there is no intense external optical field (such as a ruby laser beam) acting on this system, a great number of the molecules are in the ground state $\phi_0(t)$ with energy E_0, while only a very small number of the molecules are in the excited state $\phi_K(t)$ with energy E_k. When an external optical field is acting on this system, the potential energy function, U(R), for a molecule is changed by an amount

$$\Delta U(R;\vec{r},t) = -\frac{1}{2}\alpha(R)E(\vec{r},t)^2$$

where R is the separation between the nuclei of a molecule, $\alpha(R)$ is the polarizability, $E(\vec{r},t)$ is the optical electric field.

The time dependent Schroedinger equation for each molecule is

$$i\hbar\dot{\Psi}(R;\vec{r},t) = H(R;\vec{r},t)\Psi(R;\vec{r},t)$$

where the total Hamiltonian operator for nuclear motion is

$$H(R;\vec{r},t) = H_0(R)+H'(R;\vec{r},t)$$
$$= H_0(R)+\Delta U(R;\vec{r},t)$$

(where $H_0(R)$ is the unperturbed Hamiltonian) and the wave function $\Psi(R;\vec{r},t)$ can be expanded in terms of eigenstates of $H_0(R)$,

$$\Psi(R;\vec{r},t) = \sum_j a_j(\vec{r},t)\varphi_j(R,t)$$

with

$$i\hbar\dot{\varphi}_j = H_0\varphi_j$$

and

$$\varphi_j(R,t) = u_j(R)\exp(-i\omega_j t)$$

$$\omega_j = E_j/\hbar$$

$$H_0 u_j = E_j u_j$$

Using these relations and assuming a thermal relaxation with the form

$$\dot{a}_k = -\frac{\gamma}{2} a_k$$

we can obtain the following equation

$$\dot{a}_k = -\frac{\gamma}{2} a_k - \frac{1}{2i\hbar} E(\vec{r},t)^2 \langle\varphi_k|\alpha(R)|\varphi_0\rangle$$

where γ is the inverse lifetime, i.e. the fractional loss per unit time for $|a_k|^2$. Solving this equation we get

$$a_k(\vec{r},t) = \frac{E_L^* E_S \alpha_{k0} \exp(i\vec{k}\cdot\vec{r} + i(\omega_{k0}-\omega)t)}{4\hbar(\omega_{k0} - \omega - i\gamma/2)}$$

where $\alpha_{k0} \equiv \langle u_k|\alpha(R)|u_0\rangle$

$$E(\vec{r},t) = E_L(\vec{r},t) + E_S(\vec{r},t)$$

$$E_L(\vec{r},t) = (\tfrac{1}{2})E_L \exp(-i\vec{k}_L\cdot\vec{r} + i\omega_L t) + \text{C.C.}$$

$$E_S(\vec{r},t) = (\tfrac{1}{2})E_S\exp(-i\vec{k}_S\cdot\vec{r} + i\omega_S t) + C.C.$$

$$\vec{k} = \vec{k}_L - \vec{k}_S, \quad \omega = \omega_L - \omega_S$$

$$\omega_{k0} = \frac{E_k - E_0}{\hbar}$$

The total electric polarization per unit volume is

$$P(\vec{r},t) = N\alpha(\vec{r},t)E(\vec{r},t)$$

where $\alpha(\vec{r},t)$ is the actual molecular polarizability

$$\alpha(\vec{r},t) = \langle\Psi(R;\vec{r},t)|\alpha(R)|\Psi(R;\vec{r},t)\rangle$$

$$= \langle\varphi_0|\alpha(R)|\varphi_0\rangle + (a_k\langle\varphi_0|\alpha(R)|\varphi_k\rangle + C.C.)$$

$$+ \text{higher order terms}$$

The second terms represent the field-dependent polarizability

$$\alpha(\vec{r},t)^{(\text{field-dependent})} = a_k\alpha_{0k}\exp(-i\omega_{k0}t) + C.C.$$

$$= \frac{E_L^* E_S|\alpha_{0k}|^2\exp(i\vec{k}\cdot\vec{r} - i\omega t)}{4\hbar(\omega_{k0} - \omega - i\gamma/2)}$$

$$+ C.C.$$

Hence the nonlinear polarization at ω_S is

$$P_{NL}(\vec{r},t;\omega_S) = \frac{N|E_L|^2|\alpha_{0k}|^2}{4\hbar(\omega_{k0} - \omega - i\gamma/2)}\left[\frac{E_S}{2}\exp(-i\vec{k}_S\cdot\vec{r} + i\omega_S t)\right]$$

$$+ C.C.$$

Using the Maxwell's wave equation

$$\left(\nabla^2 - \frac{n^2}{c^2}\frac{\partial^2}{\partial t^2}\right)E(\vec{r},t) = \frac{4\pi}{c^2}\frac{\partial^2}{\partial t^2}P_{NL}(\vec{r},t)$$

where n is the index of refraction, and regarding E_S as a slowly varying spatial function, we obtain the following relation for the terms which vary as ω_S

$$\left(-k_S^2 + \frac{n^2\omega_S^2}{c^2}\right) E_S - 2i\vec{k}_S\cdot\nabla E_S = -\frac{4\pi}{c^2}\chi_{NL}(\omega_S) E_S \omega_S^2$$

where the nonlinear susceptibility $\chi_{NL}(\omega_S)$ is

$$\chi_{NL}(\omega_S) = \frac{N|E_L|^2|\alpha_{0k}|^2}{4\hbar(\omega_{k0} - \omega - i\gamma/2)} .$$

Assuming

$$k_S = \frac{n\omega_S}{c}$$

i.e. the real part of the nonlinear susceptibility $\chi_{NL}(\omega_S)$ is not important here, we obtain the gain per unit length for the scattered intensity $G_S(\omega)$

$$G_S(\omega) \equiv 2\frac{\partial E_S/\partial x}{E_S} = \frac{\pi k_S N|\alpha_{0k}|^2|E_L|^2\gamma/2}{n^2\hbar\left[(\omega_{k0}-\omega)^2 + (\gamma/2)^2\right]}$$

When $\omega = \omega_{k0}$, the gain is maximum

$$G_S(\omega = \omega_{k0}) = \frac{2\pi k_S N|\alpha_{0k}|^2|E_L|^2}{n^2\hbar\gamma}$$

where γ is the linewidth of the Raman transition.

2. Linewidth

The spectral half-intensity width γ of Raman lines observed from gases has been shown to depend on the gas density with the relation

$$\frac{\gamma}{2} = \frac{k^2 D_0}{2\pi\rho} + B\rho$$

where k is the magnitude of the wave vector difference between the incident and scattered photons, D_0 the coefficient of self diffusion at one amagat, ρ the gas density in amagats, and B the collision-broadening coefficient. For low gas densities (several amagats) in H_2 gas, γ decreases with increasing pressure, this effect is known as Dicke narrowing. The linewidth therefore has a minimum value at about 10 amagats for H_2.

An explanation of Dicke narrowing can be found in references[10],[11],[12]. Briefly, a simple explanation of the narrowing is the following: From the uncertainty principle $\Delta x \, \Delta p_x \gtrsim \hbar$, the shortest displacement which can be measured for a molecule emitting a photon of momentum h/λ is $\lambda/2\pi$. The velocity of a molecule as measured by the Doppler shift is the mean velocity component in the direction of observation for displacement larger than $\lambda/2\pi$. If a molecule has many collisions in traveling the distance $\lambda/2\pi$, its mean velocity averaged over $\lambda/2\pi$ will be greatly reduced, since collisions will take the molecule through all possible velocity states.

This reduction in the mean velocity of the molecule will reduce the Doppler broadening. Therefore, the linewidth is inversely proportional to the collision rate, i.e. inversely proportional to the gas density.

Pressure broadening can be understood as resulting from an interruption of the radiative process by collisions resulting in truncation of the emitted wavetrain. The shorter the wavetrain is, the broader the linewidth will be. Consequently, if only binary collisions are considered, the linewidth is proportional to the collision frequency and hence proportional to the density.

3. Threshold Power

The intensity of the stimulated Raman line I_S can be written as follows:

$$I_S = I_{SO}\exp(G_S - L)\ell$$

where ℓ is the length of the interaction region in the scattering medium,

$$G_S(\omega = \omega_{k0}) = \frac{2\pi k_S N \left|\alpha_{0K}\right|^2 \left|E_L\right|^2}{n^2 \hbar \gamma}$$

is the maximum gain of the stimulated Raman scattering given in Section 1, and L is the loss of the scattered intensity in the medium. From Section 2, the linewidth γ is

$$\gamma = A/\rho + B\rho \ .$$

Since N is proportional to ρ, k_S and $|\alpha_{ok}|^2$ are independent of ρ, and n^2 can be regarded as independent of ρ, the gain can be written as

$$G_S(\omega = \omega_{k0}) = C_1 f(\rho) P_L$$

where

$$f(\rho) = \frac{\rho}{A/\rho + B\rho}$$

C_1 is a proportionality constant independent of ρ, and P_L is the power of the laser beam which is proportional to $|E_L|^2$. Therefore

$$I_S = I_{S0}\exp\left[C_1 f(\rho) P_L - L\right]\ell$$

The threshold power of the stimulated Raman scattering at a given gas density is the minimum power of the laser beam which is required to produce the weakest observable intensity of this line. Therefore

$$I_{S,min.} = I_{S0}\exp\left[C_1 f(\rho)\ P_{th} - L\right]\ell = \text{constant}$$

where P_{th} is the threshold power,

$$C_1 f(\rho) P_{th} - L = \text{constant}$$

$$P_{th} = \frac{C_2}{f(\rho)}$$

where the loss L has been assumed to be independent of the gas density ρ and the laser power P_L.

We have

$$P_{th} = \frac{A'}{\rho^2} + B'$$

where $A' = C_2 A$ and $B' = C_2 B$.

CHAPTER IV

RESULTS AND DISCUSSION

In Fig. 2, typical spectrograms showing the stimulated rotational Raman $S_0(1)$ line and the stimulated vibrational Raman $Q_1(1)$ line of hydrogen are reproduced together with some emission lines of neon which were used to calibrate the spectra. Of the possible rotational Raman lines we could observe on our spectrograms, i.e. $S_0(0)$ and $S_0(1)$, only Stokes line corresponding to the $v = 0$ and $J=1\rightarrow3$ transition was observed as seen in Fig. 2(b). It is noted, however, that in "normal" hydrogen at room temperature the relative population of J=0 and J=1 states are 13.4% and 66.9%, respectively[13], $S_0(1)$ transition thus possessing the greater transition probability. The frequency shift of the stimulated Raman line from the exciting laser line is given in Table I. The value seems in good agreement with the corresponding shift observed in ordinary spontaneous Raman spectrum[14]. For the vibrational Raman lines arising from the J=0 and $v=0\rightarrow1$ transitions, only $Q_1(1)$ line corresponding to J"=1 J'=1 transition was observed. As shown in Fig. 2(a), one order of Stokes-shifted and several orders of anti-Stokes-shifted lines were present for most of the incident laser powers used, with the frequency shifts equal to exact

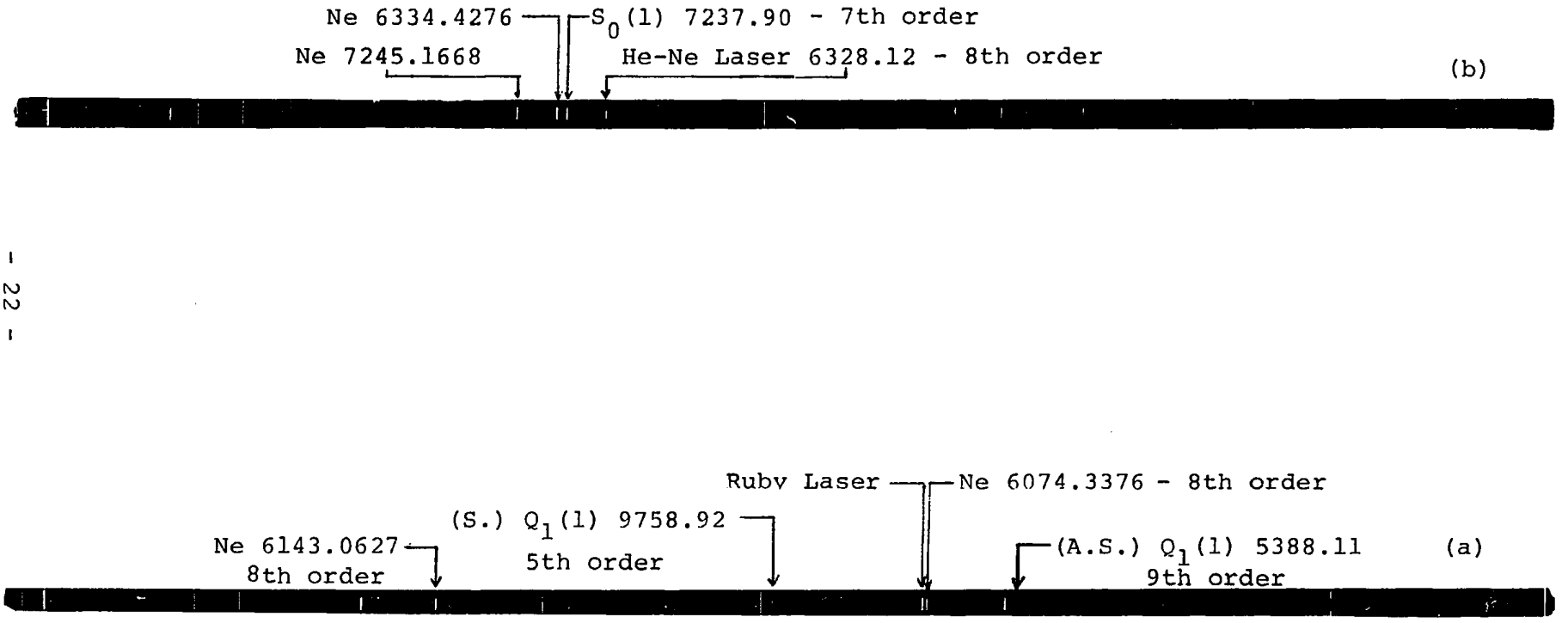

Fig. 2. Spectrogram of $Q_1(1)$, $S_0(1)$ stimulated Raman lines of H_2 and Neon standard. $S_0(1)$ line is in 7th order and Stokes $Q_1(1)$ is in 5th order.

multiples of the $Q_1(1)$ line. At threshold condition, however, only a single Stokes-shifted line was observed. The frequency shift of $Q_1(1)$ line is also given in Table I.

The following general features, some of which seem quite interesting, were observed in the production of the stimulated Raman lines:

(1) The stimulated $Q_1(1)$ line of hydrogen was observed with linearly polarized laser light at all pressures in the range 4—28 atm.

(2) No stimulated $S_0(1)$ line was observed with linearly polarized laser light at all pressures up to 28 atm and powers up to 120MW.

(3) The stimulated $Q_1(1)$ line was observable with circularly polarized laser light at all pressures in the range 7—28 atm with somewhat higher threshold powers than for (1) above. It should be noted that at pressures below 7 atm with circularly polarized light the $Q_1(1)$ line was not observable within the present power maximum, while the line was observable with linearly polarized laser light.

(4) The stimulated $S_0(1)$ line was observable with circularly polarized laser light at pressures between 3—17 atm within the present laser power maximum. Consequently, there was a well-defined "high pressure threshold" for the $S_0(1)$ line which was not present for the $Q_1(1)$ line.

TABLE I

Frequency shifts of stimulated $S_0(1)$ and $Q_1(1)$ lines of H_2

(units: cm^{-1})

	Observed Shift	Spontaneous Raman Scattering Data[14]
$S_0(1)$	587.05± 0.04	587.055
$Q_1(1)$	4156.09±0.09	4155.201

The threshold powers necessary to produce the stimulated Raman lines of hydrogen as functions of gas pressure were measured and presented in Table II.

Fig. 3 shows the threshold laser power for the stimulated vibrational Raman $Q_1(1)$ line produced by linearly polarized laser light plotted versus gas density. It is apparent from this figure that the threshold power decreases very rapidly with increasing gas density in the region of 4—12 amagats. For gas density higher than 12 amagats, the threshold power does not change much. A function of the form

$$P_{th}=A'\rho^{-2}+B'$$

as given in Chaper III was fitted to the experimental data on a P_{th} versus ρ^{-2} plot as shown in Fig. 4. Coefficients A' and B' were found to be 48.80 and 1.56 respectively by using the least square fit to all data points. The solid-line curve on Fig. 3 is $P_{th}=48.80\rho^{-2}+1.56$. These results are consistant with the results of Lallemand et al[4] at least qualitatively. It is noted, however, that they observed the gain relationship for the back-scattering.

Fig. 5 shows the variation of the threshold power for the stimulated $Q_1(1)$ line produced by circularly polarized laser light with the gas density. For densities

TABLE II

Observed Threshold Power Density Data (10^3 MW/cm^2)

Gas Density (Amagat)	$S_0(1)$ Circular Polarization	$Q_1(1)$ Circular Polarization	$Q_1(1)$ Linear Polarization
2.74	5.56	-	-
3.96	2.95	-	4.44
4.57	2.88*	-	-
6.10	3.10	3.49	3.66
8.25	2.27	2.06	-
10.70	2.51	2.23	1.82
11.61	-	-	1.22
11.92	2.39, 3.03*	1.57	-
14.37	3.58*	1.88	1.55
15.59	4.50	-	-
19.27	-	2.77	1.96
22.33	-	3.07	1.86
25.39	-	3.73	1.71

*Constant Power Series

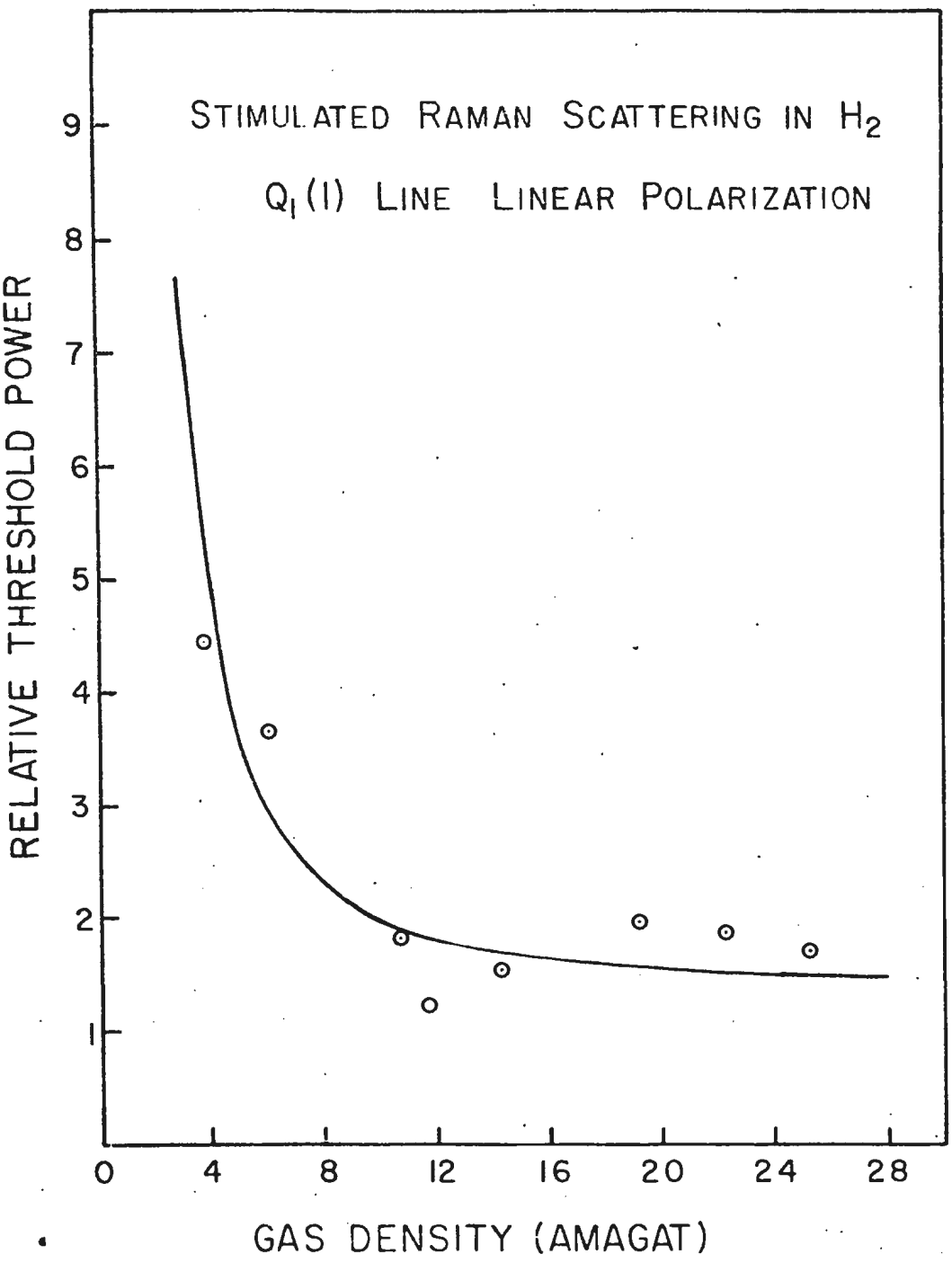

Fig. 3 SRS in H_2, $Q_1(1)$ Line, Linear Polarization, P_{th} vs. ρ

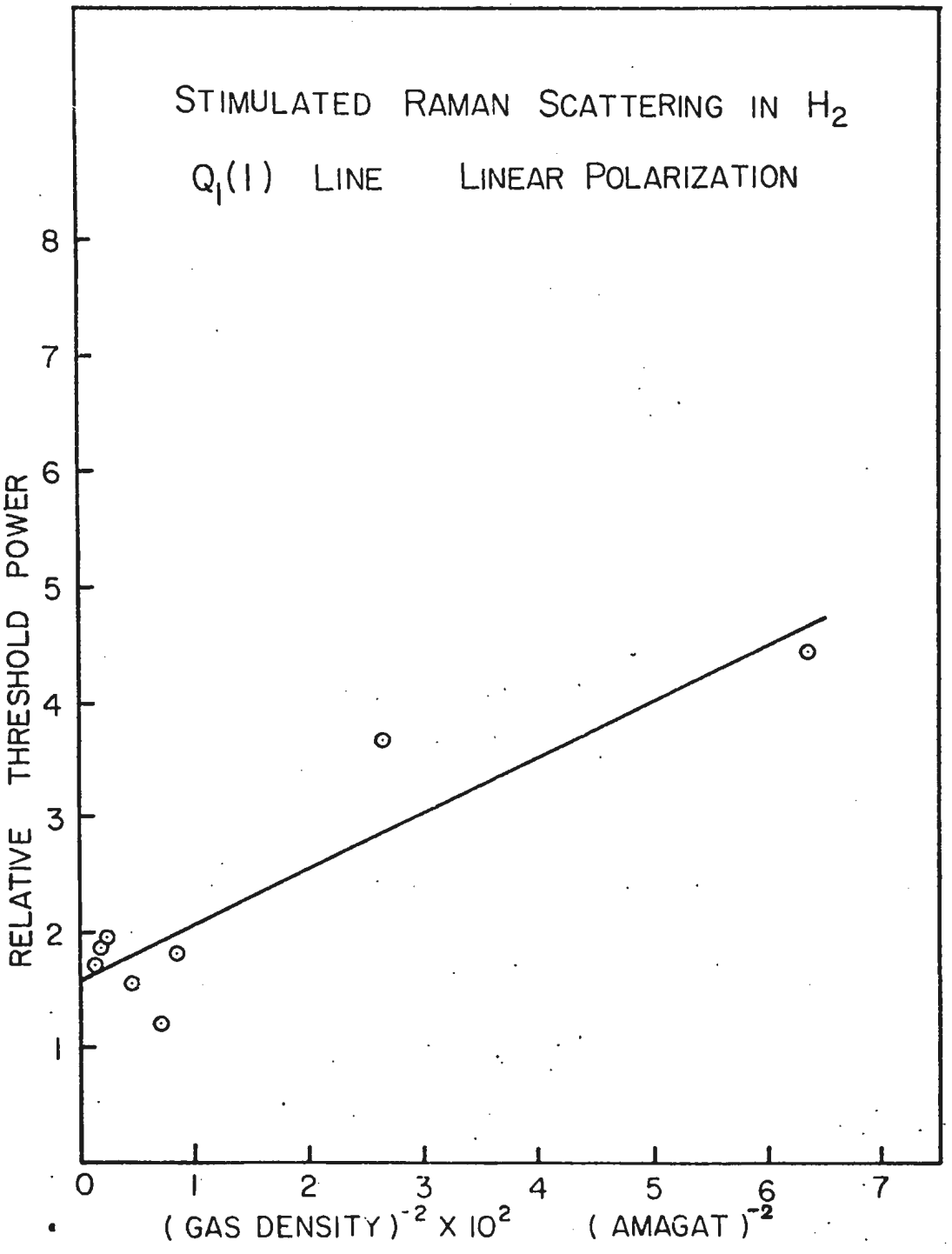

Fig. 4 SRS in H_2, $Q_1(1)$ Line, Linear Polarization, P_{th} vs. ρ^{-2}.

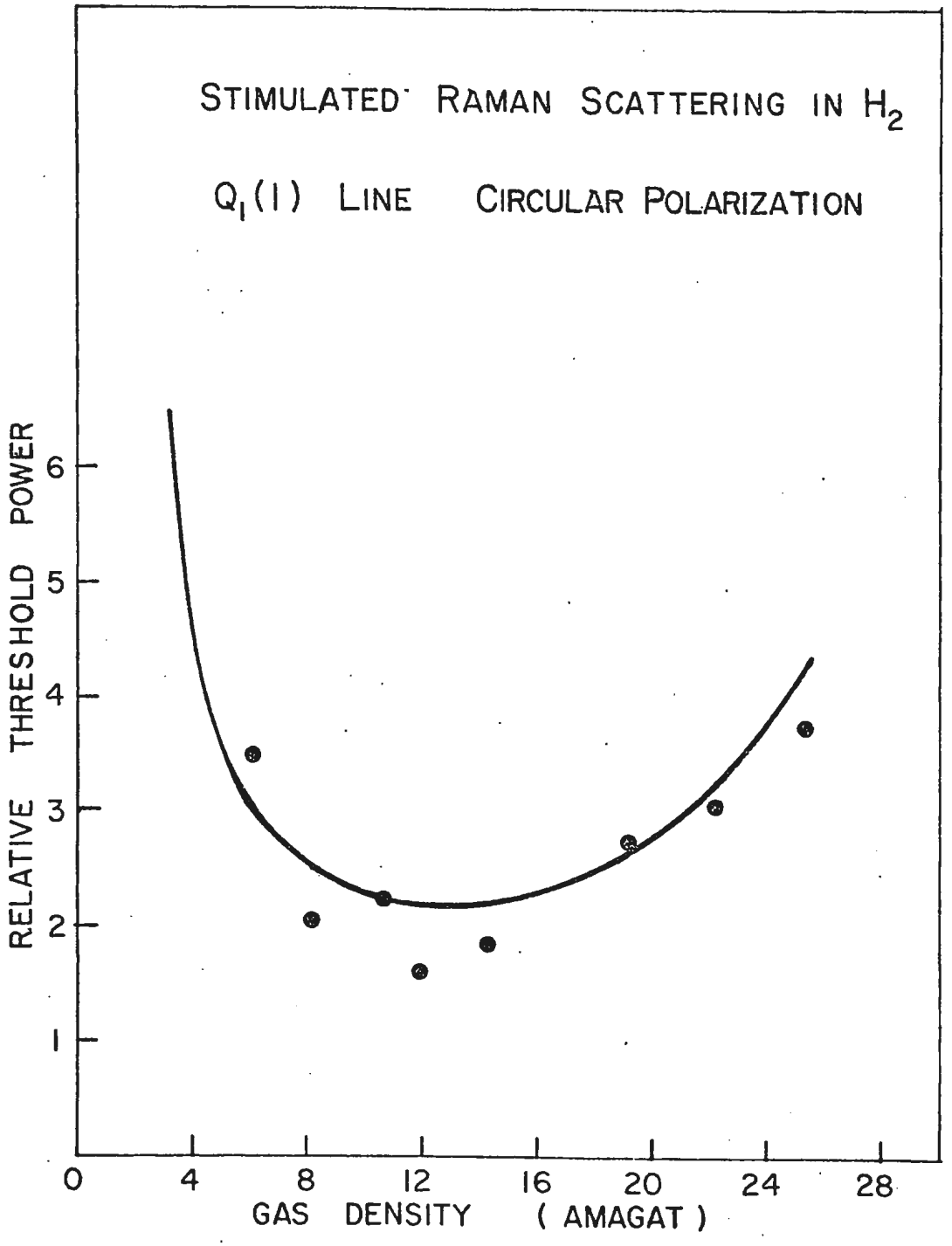

Fig. 5 SRS in H_2, $Q_1(1)$ Line, Circular Polarization, P_{th} vs. ρ^2 $C^1 = 0.00097$.

below 12 amagats, the threshold power decreases with increasing density in agreement with the case of using linearly polarized laser light, while for greater densities it appears that the threshold power is influenced by other effects dependent on the gas density. To obtain a curve to fit this data several functional forms of ρ were tried, however, the best fit to our data was obtained with a factor of $(1 - C\rho^2)^{-1}$ times $(A'\rho^{-2} + B')$, where A' and B' are the same as those for linearly polarized laser light, and C is a constant.

Such a correction factor can be deduced theoretically if one assumes another nonlinear process in the gas which competes with the stimulated Raman scattering for laser power[15]. A brief account of this effect can be given as follows: The laser power as a function of the distance into the scattering medium can be written as

$$P_L(z) = P_L(0)\ (1 + g\ P_L(0)\ z)^{-1}$$

where g is the gain for the other nonlinear process. The threshold power for the stimulated Raman scattering will then be

$$P_{th} = (A'\rho^{-2} + B')\ (1 - F(\rho)\ )^{-1}$$

where $F(\rho) = (A'\rho^{-2} + B')\ gz$.

We observed no stimulated rotational Raman lines

for the laser power available in the density range 3-25 amagats with linearly polarized laser light.

Fig. 6 shows the threshold laser power for the stimulated rotational Raman $S_0(1)$ line produced by circularly polarized laser light plotted versus gas density. The threshold power varies just as for the $Q_1(1)$ case with circularly polarized laser light, with the minimum at about 8 amagats in this case. Accordingly, we applied the same form of correction factor $(1 - C\rho^2)^{-1}$ to the expression $P_{th} = A'\rho^{-2} + B'$. The coefficients A' and B' are found by the least square fit of $P_{th} = A'\rho^{-2} + B'$ to the low density data. Fig. 7 shows the plot of P_{th} versus ρ^{-2} and a straight line of $P_{th} = A'\rho^{-2} + B'$ with A' = 28.85 and B' = 1.54. The constant C in the correction factor $(1 - C\rho^2)^{-1}$ is C = 0.00266. The curve $P_{th} = (28.85\rho^{-2} + 1.54)\ (1 - 0.00266\rho^2)^{-1}$ is shown in Fig. 6.

In conclusion, the following observations were made:

(1) Even at the maximum laser power available we did not observe the stimulated $S_0(1)$ line of hydrogen with linearly polarized incident light, this implies that the threshold power for linearly polarized incident light to produce the stimulated $S_0(1)$ line is at least 4 times the threshold power for circularly polarized incident light.

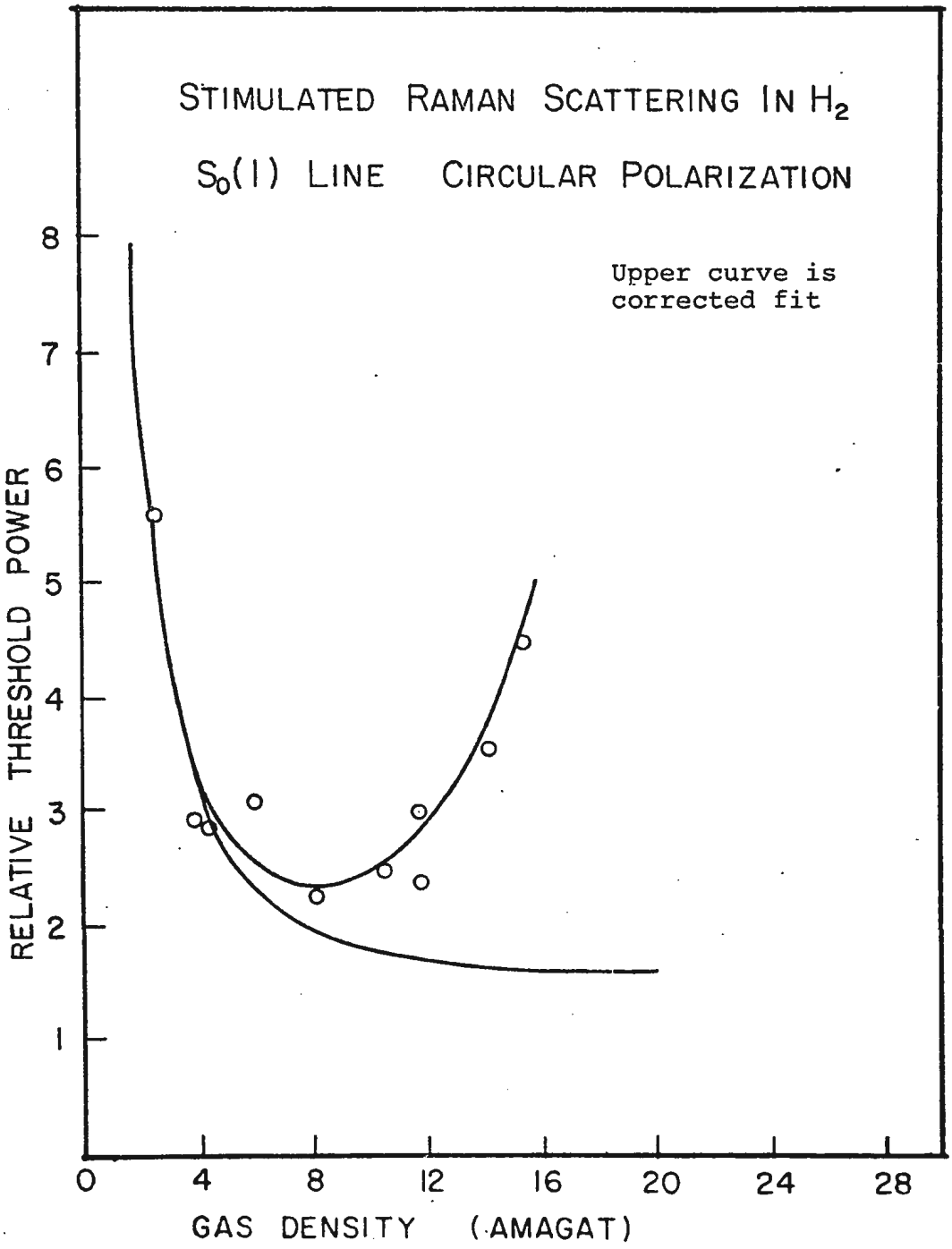

Fig. 6 SRS in H_2, $S_0(1)$ Line, Circular Polarization, P_{th} vs. ρ C = 0.00266.

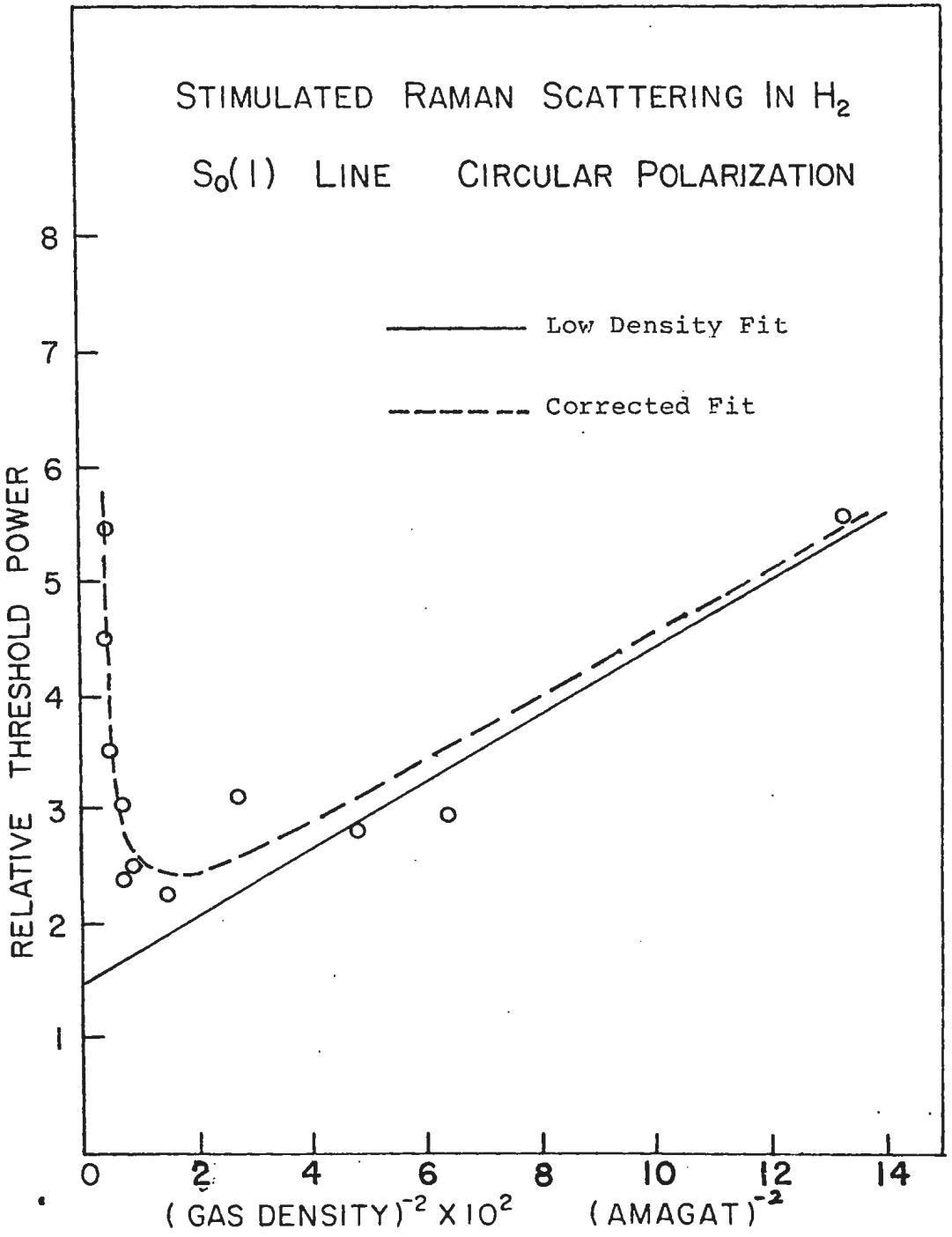

Fig. 7 SRS in H_2, $S_0(1)$ Line, Circular Polarization, P_{th} vs. ρ^{-2}

(2) The threshold power for the stimulated $Q_1(1)$ line with linearly polarized incident light was found to depend on the gas density in the form similar to that arising from the spontaneous Raman linewidth, which depends on the Dicke narrowing and pressure broadening processes. On the other hand, with circularly polarized incident light, the threshold power for both stimulated $Q_1(1)$ and $S_0(1)$ lines was found to depend on the gas density through two factors: (i) a factor similar to that observed with linearly polarized laser light, and (ii) a "correction" factor which seems to indicate the presence of other competing nonlinear process. The observed coefficients A', B' and C, defined previously, are summarized in Table III.

In order to make quantitative comparison between the linewidth factors observed by previous investigators[11],[12] and the present results, the coefficient ratio A/B is computed under various assumptions. In Table IV these computed A/B ratios are listed together with the values of A'/B' as observed. For both $Q_1(1)$ and $S_0(1)$ lines the observed A'/B' ratios do not agree with the forward or backward spontaneously scattered A/B ratios. However, when k^2 in $A = k^2 D_0/2\pi$ is replaced by the value corresponding to the average of forward and backward values, closer agreements were found between the coefficient ratios for both the $Q_1(1)$ and $S_0(1)$ lines of hydrogen.

TABLE III

Summary of observed coefficients

		A'	B'	C
$Q_1(1)$	↕	48.8	1.56	0
	↻	48.8	1.56	0.00097
$S_0(1)$		28.85	1.54	0.00266

↕ Linear polarization

↻ Circular polarization

TABLE IV

Comparison of the observed values of A'/B' with the ratios of the Dicke narrowing coefficient A to the pressure broadening coefficient B for $Q_1(1)$ & $S_0(1)$ Raman lines of H_2.

Raman Transition	Computed $A/B \equiv \frac{k^2 D_0}{2\pi B}$ from the spontaneous Raman linewidth data*			Observed Ratio A'/B'
	Back-scattered light $k^2 = (k_L + k_S)^2$	Forward-scattered light $k^2 = (k_L - k_S)^2$	Forward-backward average $\overline{k^2} = k_L^2 + k_S^2$	
$Q_1(1)$	115	3.3	59	31
$S_0(1)$	59	0.03	30	19

*$Q_1(1)$ Reference[10] $D_0 = 1.36$ cm^2/sec $B = 4.5 \times 10^7$/sec

*$S_0(1)$ Reference[9] $D_0 = 1.34$ cm^2/sec $B = 11.3 \times 10^7$/sec

SUMMARY

We investigated the stimulated vibrational Raman $Q_1(1)$ line and the stimulated rotational Raman $S_0(1)$ line of hydrogen using both linearly and circularly polarized laser beam. The threshold power of the stimulated $Q_1(1)$ line by linearly polarized laser beam was found to depend on the gas density in general agreement with theory. On the other hand, the threshold power of the stimulated $Q_1(1)$ line and of the stimulated $S_0(1)$ line by circularly polarized laser beam agreed with theory only when the effect of a competing nonlinear process with a gain dependent on gas density was included. A further study is needed to identify the competing nonlinear process.

ACKNOWLEDGEMENTS

The investigation presented in this thesis was supervised by Dr. N.D. Foltz and Dr. C.W. Cho to whom the author is greatly indebted for the close guidance and continuous encouragement during the course of the experimental work and in the preparation of this thesis.

Grateful acknowledgement is due to Dr. A.O. Creaser for his very helpful discussions.

Thanks are also due to Messrs. P. Gillard, K.S. Chang, C.J. Hsu, R. Alexander, and R. Tucker for their assistance in the experimental work and the preparation of the diagrams in this thesis.

The financial support received from Memorial University of Newfoundland in the form of fellowship is gratefully acknowledged.

The author wishes to thank Dr. S.W. Breckon and the Department of Physics for having the available facilities and co-operative personnel to have this thesis completed.

REFERENCES

1. E. J. Woodbury and W. K. Ng, Proc. IRE 50, 2367 (1963).

2. R. W. Minck, R. W. Terhune, and W. G. Rado, Appl. Phys. Letters 3, 181 (1963).

3. R. W. Minck, E. E. Hagenlocker, and W. G. Rado, Phys. Rev. Letters 17, 229 (1966).

4. P. Lallemand, P. Simova, and G. Bret, Phys. Rev. Letters 17, 1239 (1966).

5. N. Bloembergen, G. Bret, P. Lallemand, A. Pine, and P. Simova, JQE 3, 197 (1967).

6. D. H. Rank and T. A. Wiggins, J. Chem. Phys. 39, 1348 (1963).

7. C. J. Hsu, M.Sc. Thesis, Memorial University of Newfoundland, St. John's, Newfoundland, Canada, March, 1971.

8. A. Michels, W. DeGraaff, T. Wassemaar, J. M. H. Levelt, and P. Louwerse, Physica 25, 25 (1959).

9. R. M. Herman, Selected Topics in Nonlinear Optics (a series of lectures), Dept. of Physics, The Pennsylvania State University, University Park, Pennsylvania, U.S.A.

10. R. H. Dicke, Phys. Rev. 89, 472 (1953).

11. V. G. Cooper, A. D. May, E. H. Hara, and H. F. P. Knapp, Can. J. Phys. 46, 2019 (1968).

12. J. R. Murray and A. Javan, J. Mol. Spect. 42, 1 (1972).

13. K. S. Chang, M.Sc. Thesis, Memorial University of Newfoundland, St. John's, Newfoundland, Canada, January 1971.

14. B. P. Stoicheff, Can. J. Phys. 35, 730 (1957).

15. R. W. Minck, E. E. Hagenlocker, and W. G. Rado, J. Appl. Phys. 38, 2254 (1967).